

# Time-resolved multi-omics illustrates host and gut microbe interactions during *Salmonella* infection.

*Yongseok Kim, Katherine Kokkinias, Anice Sab-Daigle, Ikaia Leleiwi, Mikayla Borton, Michael Shaffer, Maryam Baniasad, Rebecca Daly, Brian M.M. Ahmer, Kelly C. Wrighton, Vicki H. Wysocki*

Yongseok Kim, The Ohio State University, Department of Chemistry and Biochemistry,  
Columbus, Ohio, United States

Katherine Kokkinias, Colorado State University, Department of Microbiology, Immunology, and  
Pathology, Fort Collins, Colorado, United States

Anice-Sabag-Daigle, The Ohio State University, Department of Microbial Infection and  
Immunity, Columbus, Ohio, United States

Ikaia Leleiwi, Colorado State University, Department of Cell & Molecular Biology, Fort Collins,  
Colorado, United States

Mikayla Borton, Colorado State University, Department of Soil and Crop Sciences, Fort Collins,  
Colorado, United States

Michael Shaffer, Colorado State University, Department of Soil and Crop Sciences, Fort Collins,  
Colorado, United States

Maryam Baniasad, The Ohio State University, Department of Chemistry and Biochemistry,  
Columbus, Ohio, United States

Rebecca Daly, Colorado State University, Department of Soil and Crop Sciences, Fort Collins,  
Colorado, United States

Brian M.M. Ahmer, The Ohio State University, Department of Microbial Infection and  
Immunity, Columbus, Ohio, United States

Kelly C. Wrighton, Colorado State University, Department of Soil and Crop Sciences, Fort  
Collins, Colorado, United States

Vicki H. Wysocki, The Ohio State University, Department of Chemistry and Biochemistry and  
and Resource for Native Mass Spectrometry Guided Structural Biology, Columbus, Ohio, United  
States

**KEYWORDS.** Salmonella, multi-omics, metabolomics, lipidomics, meta-transcriptomics, mass  
spectrometry

## ABSTRACT

*Salmonella* infection, also known as Salmonellosis, is one of the most common food-borne illnesses. *Salmonella* infection can trigger host defensive functions, including an inflammatory response. The provoked-host inflammatory response has a significant impact on the bacterial population in the gut. In addition, *Salmonella* competes with other gut microorganisms for survival and growth within the host. Compositional and functional alterations in gut bacteria occur because of the host immunological response and competition between *Salmonella* and the gut microbiome. Host variation and the inherent complexity of the gut microbial community make understanding commensal and pathogen interactions particularly difficult during a *Salmonella* infection. Here we present metabolomics and lipidomics analyses along with 16s rRNA sequence analysis, revealing a comprehensive view of the metabolic interactions between the host and the gut microbiota during *Salmonella* infection in a CBA/J mouse model. We found that different metabolic pathways were altered over the four investigated time points of *Salmonella* infection (days -2, +2, +6, and +13). Furthermore, metatranscriptomics analysis integrated with metabolomics and lipidomics analysis facilitated an understanding of the heterogeneous response of mice depending on the degree of dysbiosis.

## Introduction

*Salmonellosis*, caused by *Salmonella* infection, is regarded as one of the most widely spread bacterial diseases and it usually induces inflammation in the gut resulting in diarrhea, fever, and nausea.<sup>1</sup> One of the notable impacts of *Salmonella* infection on the host is an alteration of the gut microbiota composition. Several studies have demonstrated that the host is dependent on gut

microbes for maintaining health and homeostasis. The gut bacteria contribute to the host in multiple ways, including nutrient metabolism, xenobiotic metabolism, immune system development/function, and protection from pathogens.

The symbiotic relationship between the gut microbiome and the host can be disrupted as a result of *Salmonella* infection.<sup>2,3</sup> The *Salmonella*-induced inflammatory response has the potential to disturb the balance of the gastrointestinal ecosystem, perhaps resulting in changes to the structure and abundance of microbial communities.<sup>2-4</sup> The gut microbiome has the capacity to exert an impact on *Salmonella* colonization through resource competition and the synthesis of antibiotic compounds.<sup>5-8</sup> Moreover, the immune response triggered by the invasion of *Salmonella* in hosts may potentially have detrimental consequences on the normal microbial communities, leading to elevation and/or depletion of the gut microbiota. The observed effects are attributed to the production of antibacterial compounds and the activation of the immune system.<sup>9,10</sup>

This study employed a non-targeted multi-omics approach (metabolomics, lipidomics, metagenomics, metatranscriptomics) to examine the fecal samples of CBA/J mice at multiple points of *Salmonella* infection. The objective of this study was to examine the functional consequences of *Salmonella* infection on both the composition of the intestinal microbiota and the metabolic processes occurring in the host's intestines. First, we performed untargeted metabolomics and lipidomics using liquid chromatography coupled with high resolution mass spectrometry to study differential abundance of the metabolome and lipidome at multiple time points of *Salmonella* infection. We also investigated gut microbial composition shifts in the gut induced by *Salmonella* infection by 16S rRNA sequencing. A correlation study was performed to investigate the causal association between the composition of gut microbiota and metabolism by comparing 16s rRNA sequencing with untargeted metabolomics and lipidomics. Furthermore, we

used meta-transcriptomics to assess the functional activity of the gut microbiome during *Salmonella* infection. The utilization of metatranscriptomics enables the discernment of alterations in functional profiles in relation to the level of *Salmonella* infection. The utilization of an integrative approach involving metagenomics, metatranscriptomics, metabolomics, and lipidomics enabled a more thorough understanding of the diverse regulatory mechanisms that govern different molecular phenotypes. This approach specifically illuminated the intricate relationship between the gut microbiome and *Salmonella*, particularly in terms of their interaction with carbon and energy sources.

## **Materials and methods**

### **Chemicals and reagents**

Acetonitrile, formic acid, methanol, and isopropanol were obtained from Fisher Scientific (MA, USA). All the other chemicals (dichloromethane and ammonium formate) were obtained from Sigma Aldrich (MI, USA).

### **Sample collection**

CBA/J mice were obtained from The Jackson Laboratory (ME, USA), fed on normal chow (fat (5.8%), fiber (18.3%), formula 7012) from Teklad Diets (WI, USA), and inoculated with  $10^9$  colony-forming units of *Salmonella* on Day 0. Fecal samples were collected from 40 mice for 17 days, including 3 days pre-infection. Eleven mice consisting of 4 high responder mice (high inflammation, *Salmonella* relative abundance of at least 25% for two days) and 7 low responder mice (less than 25%) at 4 timepoints were selected for this study: Day-2 (pre-infection) is the control group, and Day+2 (early), Day+6 (mid), and Day+13 (late) are the post-infection groups.

Details about the high responders and low responders are described below. After fecal sample collection, the fresh fecal pellets were flash-frozen in liquid nitrogen within a minute. Mouse experiments in this study were performed according to protocols approved by The Ohio State University Institutional Animal Care and Use Committee (IACUC). (IACUC protocol: 2009A0035-R4)

### **Sample preparation for metabolomics and lipidomics**

Individual fecal samples were used for the metabolomics and lipidomics study, and 1 mL of a solution composed of three different solvents (water/methanol/dichloromethane, 1/2/3, v/v/v) was used for biphasic extraction of metabolites and lipids, followed by physical disruption with a sonicator (Bioruptor®, Diagenode, Belgium). The disrupted fecal suspension was vortexed and incubated at room temperature. The two phases were separated, the organic layer was transferred for lipidome analysis, and the aqueous layer was used for metabolome analysis. A quality control (QC) sample was prepared by mixing an equal volume of each of the 11 samples (one per mouse). Both the organic layer and aqueous layers were analyzed with an Ultimate 3000 liquid chromatograph coupled to a Thermo Q-Exactive Plus mass spectrometer (Thermo Fisher Scientific, CA, USA) For lipidome analysis, reverse phase separation with a C18 column (ACQUITY UPLC® HSS T3 1.8  $\mu\text{m}$ , 2.1 x 100 mm, Waters Corporation, MA, USA) was applied for liquid chromatography separation. The mobile phase consisted of water/acetonitrile (6/4, v/v) for solvent A and water/acetonitrile/isopropanol (2/2/6, v/v/v) for solvent B, both of which contained 0.1 % (v/v) formic acid and 10 mM ammonium formate. A flow rate of 0.270 mL/min was used with a gradient as follows: 32% B for 0–1.5 min, from 32% B at 1.5 min to 45% B for 2.5 min, to 52% B for 1 min, to 55% B for 1 min, to 60% B for 3 min, to 70% B for 3 min, and

98% B at 19 min, then returning to the initial gradient conditions (32% B) followed by re-equilibration for 10 min. A top 8 data-dependent acquisition (DDA) method with collision-induced dissociation was applied to scan precursor and product ions in positive and negative modes. For metabolome analysis, 2 different separation methods, reverse phase liquid chromatography and hydrophilic interaction liquid chromatography (HILIC), were applied. The mobile phases for reverse phase separation consisted of water with 0.1% (v/v) formic acid (solvent A) and acetonitrile with 0.1% (v/v) formic acid (solvent B). The flow rate was set at 0.3 mL/min with the gradient as follows: 2% B for 0-2 min, from 2% B to 30% B for 4 min, to 50% B for 8 min, and 98% B for 1.5 min and held at 98% B for 1 min, then returning into initial gradient for equilibrium for 1.5 min. For HILIC separation, an ACQUITY UPLC® BEH HILIC 1.7  $\mu\text{m}$  (2.1 X 150 mm) column was used. Water/acetonitrile (95/5, v/v) with 0.1% formic acid and 10 mM ammonium formate and water/acetonitrile (5/95, v/v) with 0.1% formic acid and 10 mM ammonium formate were prepared as solvent A and solvent B respectively. For gradient elution, 99% B was held for 2 min, gradually reduced to 75% B for 7 min and reduced again to 45% B for 5 min. And the gradient was held at 45% B for 2 min, returned to the initial gradient and re-equilibrated for 5 min. The flow rate was set at 0.3 mL/min. The QC sample was analyzed after every 6 samples.

### **Data processing for metabolomics and lipidomics**

For data processing including peak detection, adduct identification () and metabolome/lipidome annotation, the collected MS data were processed with MS-Dial (v.4.90).<sup>11</sup> Any features with more than 25% relative standard deviation in QC samples were excluded to remove features with low reproducibility. The nomenclature rules for lipid species and lipid classification were applied

following MS-Dial and LIPID MAPS nomenclature.<sup>11,12</sup> All statistical results for each compound and abbreviation of the lipids are illustrated in Supporting information 1 & 2.

### **Metabolomics/lipidomics driven pathway analysis**

The pathway analysis with identified metabolites/lipids was performed using the web-based tool Metaboanalyst 5.0 (metaboanalyst.ca).<sup>13</sup> Metabolic pathways consisting of less than 2 metabolites or an impact score of less than 0.1 were excluded.<sup>14</sup>

### **16s rRNA amplicon sequencing**

Total nucleic acids were extracted from feces of each single mouse using the Quick-DNA Fecal/Soil Microbe Microprep Kit (Zymo Research, CA, USA) and stored at  $-20\text{ }^{\circ}\text{C}$  until sequencing. DNA was submitted for amplicon sequencing at the Argonne National Lab Next Generation Sequencing facility using Illumina MiSeq with  $2 \times 251$  bp paired end reads following established HMP protocols.<sup>15</sup> Briefly, universal primers 515F and 806R were used for PCR amplification of the V4 hypervariable region of the 16S rRNA gene using 30 cycles. The 515F primer contained a unique sequence tag to barcode each sample. Both primers contained sequencer adapter regions. Data was processed using Qiime2 2021.4.0 with specific steps described here.<sup>16</sup> In short, raw data fastq files were demultiplexed and amplicon sequence variants (ASVs) were chosen using DADA2 and assigning taxonomy via SILVA release 138 SSU Ref NR 9917.

### **Integration of 16s rRNA and metabolomics/lipidomics**

To explore the compositional relationship between fecal metabolites/lipids with gut microbes during *Salmonella* infection, we calculated the statistical correlation between the gut microbial

abundance from 16S rRNA sequencing and the chromatographic area of metabolites/lipids. The gut microbes identified in less than 20% of the samples were excluded, and 46 gut microbes were selected for further analysis. Pseudo count (1E-9) was added before centered log-ratio transformation (CLRT). CLRT was also applied to the LC-MS data to reduce the effect of the different response magnitudes from the two acquisition modes. Pearson coefficient was calculated with two centered log-ratio transformed data.<sup>18</sup>

### **Metatranscriptomics analysis**

Total RNA was extracted using the ZymoBIOMICS DNA/RNA Miniprep Kit (Zymo Research, CA, USA) and stored at  $-80^{\circ}\text{C}$  until sequencing. RNA for meta-transcriptomics was submitted to a facility at the University of Colorado-Denver and the sequencing library was prepared using the Zymo-Seq RiboFree Total RNA Library Kit (Zymo Research, CA, USA). Libraries were quantified and then sequenced on the NovaSeq 6000 using paired-end 150-bp reads (2x150) on an S4 flow cell (v1.5 chemistry). Reads were trimmed and had adapters removed using bbdduk (v38.89) and mapped to a custom genome database including the dereplicated set from the CBAJ-DB and additional metagenome assembled genomes (MAGs) from additional metagenomic sequencing of CBA/J mice fed high-fat diet or chow per methods previously described (total of 141 MAGs) using bowtie2 (v2.4.5).<sup>19,20</sup> Counts were then generated using htseq (v21.0.1) and normalized using DESeq2 or geTMM in R.<sup>21-23</sup> Groups for DESeq2 normalization were selected based on high or low responder status as determined by *Salmonella* relative abundance.

## **Results and discussion**

### **Investigation of the temporal dynamics of *Salmonella* abundance**

The abundance of *Salmonella* was measured using 16S rRNA analysis for samples collected over a period of 18 days, encompassing 3 days prior to the inoculation of *Salmonella* and 15 days following the inoculation (Figure S1). We divided the mice into two groups based on the prevalence of *Salmonella* over time: high responder (HR) mice and low responder (LR) mice. HR mice are classified as mice with *Salmonella* relative abundance  $\geq 25\%$ , detected in at least 2 time points in a minimum of two time periods, while all other mice were categorized as LR mice. There were 6 high responder mice and 34 low responder mice. To examine the effects of *Salmonella* infection on gut metabolisms across an infection time course, we selected 4 HR mice (out of 6 HR mice, because there were insufficient fecal samples for 2 of the HR mice) and 7 LR mice (out of 34 LR mice) at three post-infection time points (Day+2: "Early", Day+6: "Mid", and Day+13: "Late") and one pre-infection time point (Day-2) for metabolomics/lipidomics analysis. The four HR mice (M1, M2, M3, and M4) exhibited a steady increase in *Salmonella* abundance over time, but the seven LR mice (M5, M6, M7, M8, M9, M10, and M11) did not (Figure 1).

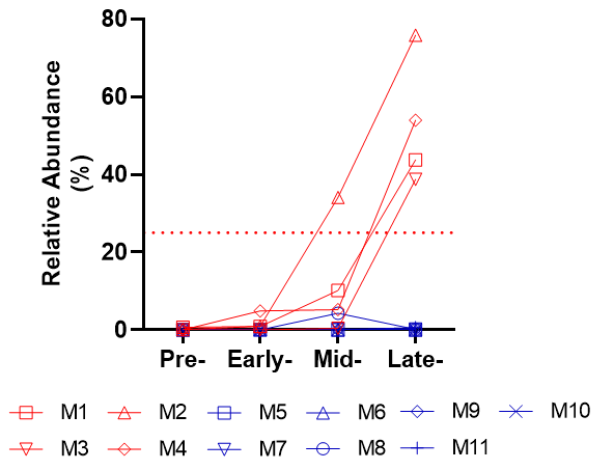


**Figure 1.** The relative abundance changes of the family of *Enterobacteriaceae* (indicating *Salmonella*) in 11 CBA/J mice. The red dotted line indicates a *Salmonella* abundance of 25%, the definition of high responder in this study.

### Overview of the gut metabolome/lipidome analysis and the gut microbe abundance analysis

Principal component analysis (PCA) was performed to see whether *Salmonella* infection traits could be discriminated at different time points in the metabolomics and/or lipidomics data. Figures 2A through 2F display PCA score plots for lipidomics and metabolomics. For the lipidomics data, we did not find any distinct separation between the pre-infection and early post-infection groups but there was a clear separation by mid and late infection. In metabolomics analysis, the distinction between the mid and late time points vs. pre- and early time points was less apparent, except for the HR mice at the late time point. At the late time point, both metabolomics and lipidomics analyses revealed that all HR mice were distinguishable from LR mice. A non-metric multidimensional scaling (NMDS) study depicting the variance in gut microbial abundance after *Salmonella* infection also revealed the considerable differences between the HR and LR groups at the late time point and these results suggest that the variation in gut microbial composition during *Salmonella* infection may have a major impact on metabolite and lipid alterations (Figure 2G). As depicted in Figure 2H, *Clostridia* and *Bacteroidia* classes account

for more than 90 percent of the composition of gut microbes prior to *Salmonella* invasion. These classes remained the predominant gut microorganisms in LR mice infected with *Salmonella*. The HR group, on the other hand, had a drastically higher abundance of *Gammaproteobacteria*, the family of bacteria associated with *Salmonella*. In the LR group, the change in the *Gammaproteobacteria* class was insignificant.

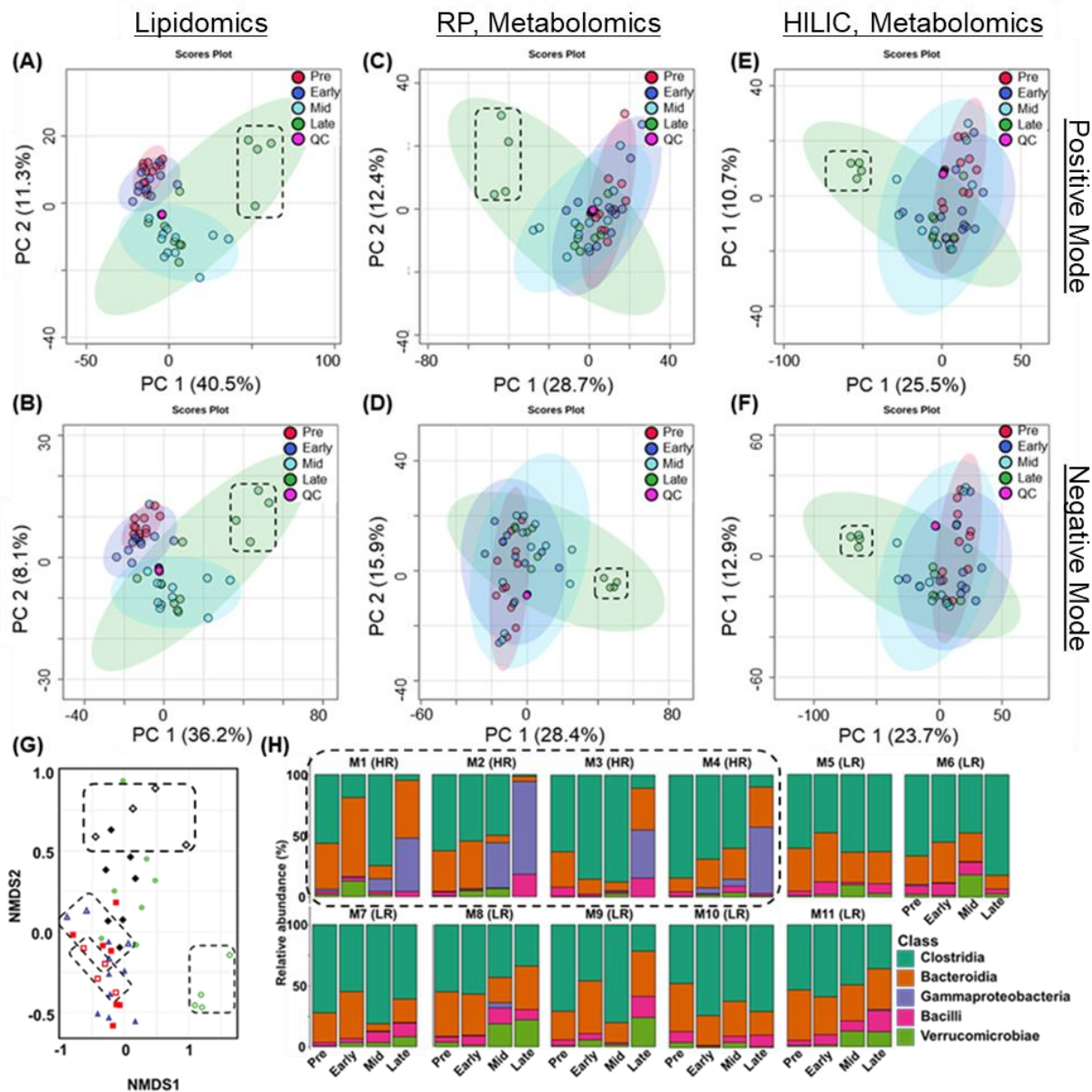


**Figure 2.** Principal component analysis of LC-MS-based lipidomics and metabolomics. Lipidomics analysis with positive (A) and negative (B) modes, metabolomics analysis with reverse-phase separation ((C): positive mode and (D): negative mode) and HILIC separation ((E): positive mode and (F): negative mode) are illustrated. The NMDS analysis from 16S rRNA analysis is shown in (G). In (G), the circles denote low responders while the diamonds denote high responders. The red, blue, black, and green colors, respectively, stand for the pre, early, mid, and late time points. The alterations of the gut microbiome in all mice are illustrated in (H) and the samples within the dashed-lined box represent the high responders in the late time point.

## Exploration of altered metabolites/lipids at multiple time points after *Salmonella* inoculation

With LC-MS-based metabolomics and lipidomics analyses, a total of 1135 compounds were identified. There are 58 lipid ontologies and 19 lipid subclasses for the identified lipids. Triacylglycerol (TG, n = 105), diacylglycerol (DG, n = 68), glycerophosphatidyl choline (PC, n = 42), and ether-linked PC (n = 36) were the most identified classes of lipids. Included within the annotated metabolites are amino acids, polyphenols, and dipeptides. Figure 3 illustrates significant alterations in metabolites and lipids following *Salmonella* infection compared to the pre-infection group. At the early infection timepoint (relative to pre-infection), six and twelve compounds were significantly elevated in LR and HR mice, respectively and 11 and 30 compounds, respectively, were decreased in LR and HR mice. Comparing the pre-infection group to the mid time point, 47 compounds showed lower abundance and 164 compounds showed higher abundance in LR mice, while 118 compounds were decreased and 241 compounds were increased in HR mice. Twenty-two and 125 compounds decreased and increased respectively, in both LR and HR mice. At the late time point of *Salmonella* infection, the number of compounds decreased in LR mice was 71, while in HR mice it was 207, compared to the pre infection time point. On the other hand, 241 and 342 compounds were elevated in both LR and HR mice.

Compounds that decreased at mid and late time points compared to pre infection group include esterified deoxycholic acid (DCAEs), sulfonolipids (SLs) and N-acyl glycines (NAGlys). The abundance of DCAEs decreased at both mid- and late time points of *Salmonella* infection in LR and HR groups (Fold change: 0.079 and 0.238 in HR and LR groups, respectively, at the mid time point, and 0.040 and 0.307 in HR and LR groups, respectively, at the late time point). The decrease in DCAEs with *Salmonella* infection is interesting in the context of prior studies indicated that dysregulation of secondary bile acid metabolism occurs in cases of intestinal microbiota

imbalances associated with diseases such as ulcerative colitis and colorectal cancer.<sup>24,25</sup> It is well known that gut microorganisms produce the esterified form of bile acids. The major bile acids secreted by the host liver are susceptible to transformation by bacteria in the gastrointestinal system. Gut microbes are capable of esterification, deconjugation, epimerization, and oxidation of bile acids.<sup>26,27</sup> We also observed that the levels of three secondary bile acids (taurodeoxycholic acid, deoxycholic acid, and hyodeoxycholic acid) exhibit a significant reduction in all mice, with a more pronounced decrease observed in the HR mice at the late time point of *Salmonella* infection. The observed alterations in bile acid metabolism can be attributed to two potential factors. First, during infection, the microbial community undergoes a shift, resulting in a decrease in the abundance of bacteria that produce secondary bile acids. Second, it is possible that the bacteria alter their behavior during infection, leading to a reduced production of secondary bile acids.

SLs are also significantly decreased in both LR and HR groups, especially at the late time point (Fold change: 0.213 in HR group and 0.348 in LR group at the late time point). SLs are known to be produced by intestinal bacteria,<sup>28,29</sup> including the *Alistipes* genre, and our 16s rRNA result indicating a decrease in the abundance of *Alistipes*, supporting a decrease in the concentration of SLs following *Salmonella* infection.<sup>29</sup> NAGlys are examples of compounds lowered in the mid-time and late-timepoint group, especially in HR mice (Fold-change: 0.128 at mid time point and 0.179 at late time point in HR group). NAGlys are also known as the microbial metabolites that contribute to cholesterol metabolism.<sup>30</sup>

Cholesteryl esters (CEs) are a class of compounds substantially elevated at the mid and late time points of *Salmonella* infection (Fold-change: 6.86 in HR group and 2.59 in LR group, respectively, at the mid time point; 12.3 and 5.77 in HR group and LR group, respectively, at the late time point). Esterification of cholesterol is a common biological process used to store,

transport, and reduce the toxicity of excess cellular cholesterol. A recent study has also indicated that dysbiosis has the potential to trigger cholesterol esterification.<sup>31</sup> The presence of significant amounts of ceramides has the potential to disrupt the microbial composition, leading to dysbiosis and this dysbiosis, in turn, triggers the activation of the cholesterol esterification pathway.<sup>32</sup> In our study, an increase in ceramide concentrations was observed after *Salmonella* infection. Hence, ceramides induced dysbiosis, has the potential to enhance the process of cholesterol esterification. Also, compounds such as glycerophosphatidylcholines (PCs) and lysoglycerophosphatidylcholines (LPCs) were significantly elevated at the late-time point group especially in HR mice (Fold change of PCs: 2.66 and LPCs: 5.14) compared to the pre-infection group. PCs and LPCs are a critical component of the membranes of epithelial cells, thus it is probable that inflammation caused by *Salmonella* infection harmed the mucosal epithelium and led to epithelial cell necrosis, which may explain the elevated PC levels.<sup>33-36</sup> Glycerophospholipids are also involved in the structural components of the cellular membrane and play a key role in many cellular processes.<sup>33</sup> PCs and LPCs also serve as cofactors required for pathogenicity of infectious organisms such as *Salmonella*.<sup>35,37</sup> Biliverdin, involved in the heme catabolic pathways, including production of urobilinogen, was also elevated at the mid and late time point of *Salmonella* infection in both HR (Fold-change: 4.69 at mid time point, 4.58 at the late time point) and LR (Fold-change: 2.93 at mid time point and 4.94 at the late time point) groups. Gut microbes are expected to participate in the urobilinogen synthesis pathway; however, bilirubin accumulated with *Salmonella* infection, suggesting that biliverdin was not converted into urobilinogen due to a disturbed gut microbial composition.<sup>38</sup> A similar result was observed in a gut-related disease, ulcerative colitis.<sup>24</sup>

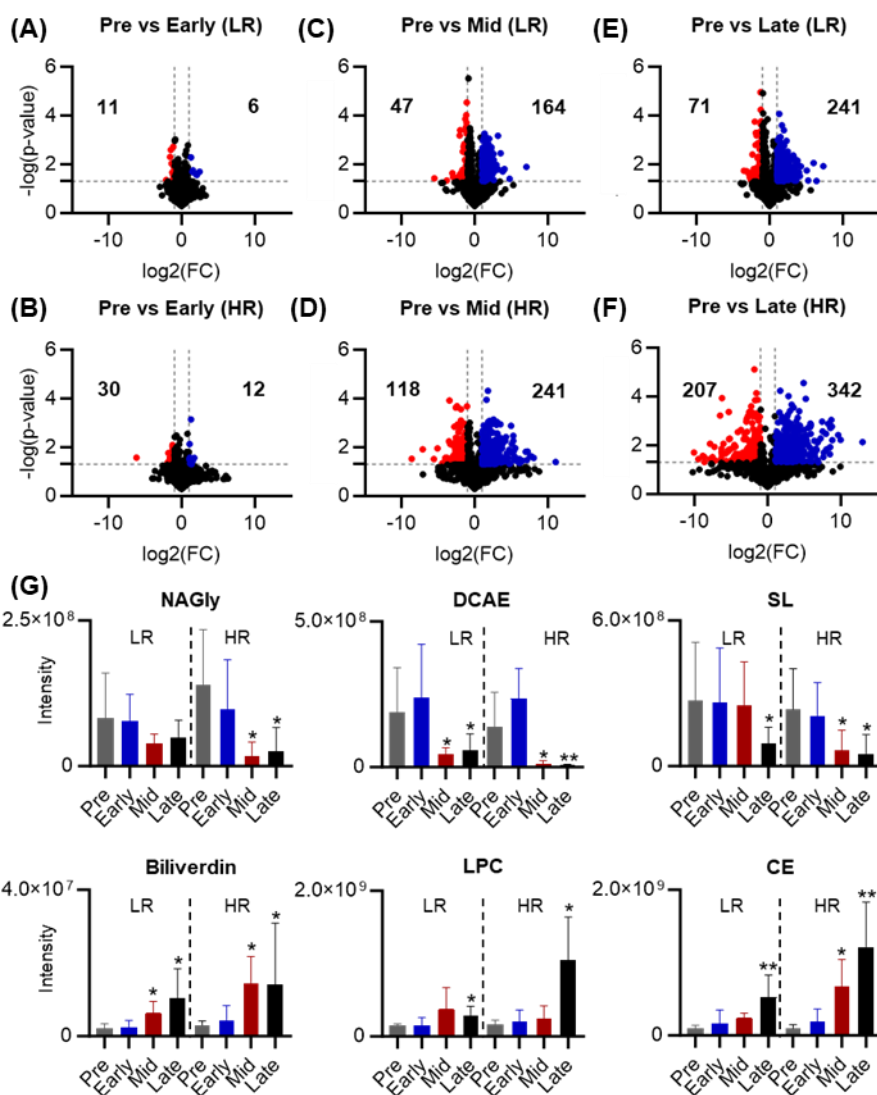


**Figure 3.** The metabolites/lipids altered compared to the pre-infection group. (Early time point: (A) LR and (B) HR; Mid time point: (C) LR and (D) HR; late time point: (E) LR and (F) HR. (G) Examples of significantly altered metabolites of *Salmonella* infection. (\*:  $p$ -value  $< 0.05$ , \*\*:  $p$ -value  $< 0.01$ , \*\*\*:  $p$ -value  $< 0.001$ )

### Metabolomics/Lipidomics driven pathway analysis

We performed pathway analysis to determine the host metabolic pathways altered by *Salmonella* infection at multiple time points compared to the pre-infection group. A total of 281 (lipids with different carbon length were considered as one compound) of our 1135 compounds were found in

the Kyoto Encyclopedia of Genes and Genomes (KEGG) compound database and pathway analysis was performed. As might be predicted, during early *Salmonella* infection, only one metabolic pathway change was seen in HR (ether lipid metabolism) and LR (pentose and glucuronate interconversions) groups. At the midpoint of *Salmonella* infection, seven metabolic pathways were significantly altered in both HR and LR groups, including sphingolipid metabolism, alanine, aspartate, and glutamate metabolism, glycerophospholipid metabolism, and ether lipid metabolism. At the late time point of *Salmonella* infection, 14 metabolic pathways were significantly altered in both the HR and LR groups, and 6 of these metabolic routes (sphingolipid metabolism, alanine, aspartate, and glutamate metabolism, glycerophospholipid metabolism, arachidonic acid metabolism, ether lipid metabolism, and arginine biosynthesis) were identified as significant pathways at both the mid and late time points. Tryptophan metabolism, arginine and proline metabolism, cysteine and methionine metabolism, galactose metabolism, amino sugar and nucleotide sugar metabolism, purine metabolism, glyoxylate and dicarboxylate metabolism, and primary bile acid biosynthesis were identified as significant metabolic pathways at the late time point. Additionally, a total of 22 metabolic pathways were identified to exhibit statistically significant variations between the HR and LR groups at the late time point. One of interesting pathways significantly different between the HR and LR groups is tryptophan metabolism ( $p$ -value  $< 0.0001$ ) as the tryptophan metabolism is highly affected by the metabolism of gut microbiome. And the high variation of gut microbiome composition/function led to influence on the host's tryptophan metabolism. More detailed information is described below. (Table S2, Figure 4)

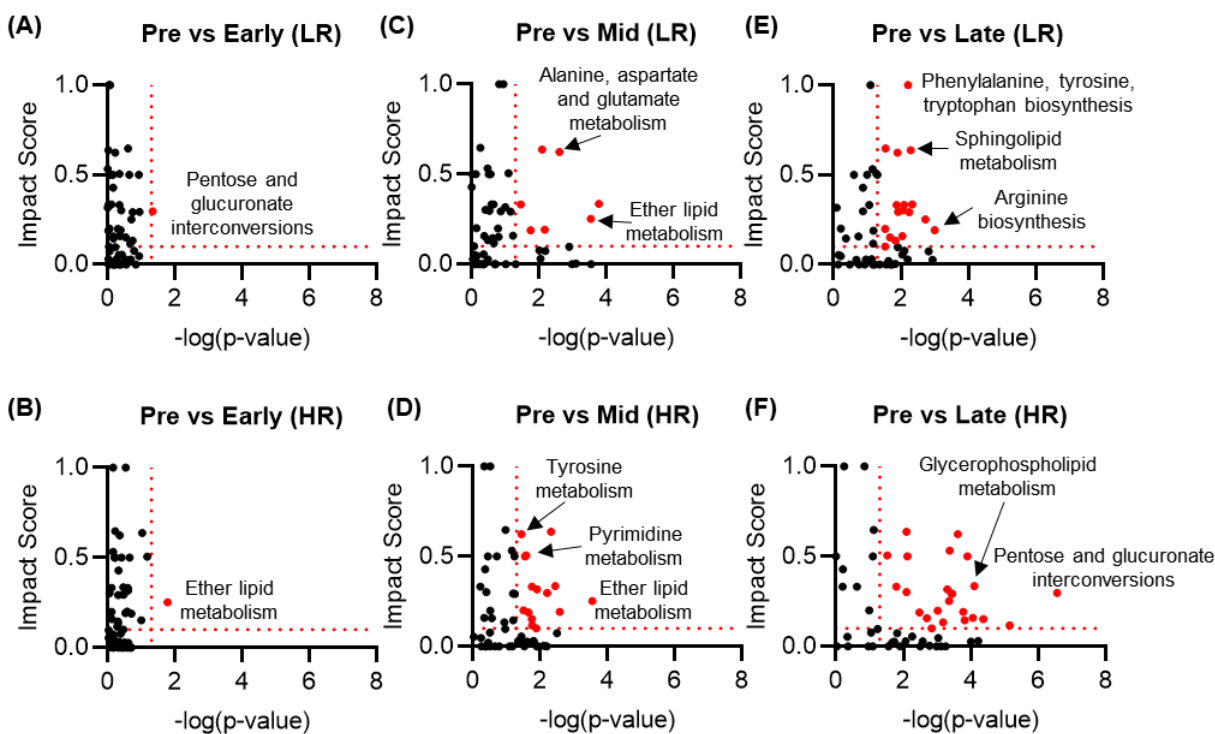


**Figure 4.** The significant host metabolic pathways at each time point *Salmonella* infection. (Early time point: (A) LR and (B) HR, Mid time point: (C) LR and (D) HR, late time point: (E) LR and (F) HR). The significantly altered metabolites at mid time point (G) and late time point (H) of *Salmonella* infection.

### Correlation of 16s rRNA analysis and metabolomics/lipidomics

Correlation of metabolomics/lipidomics and microbiota 16S rRNA amplicon sequencing relative abundance revealed a strong relationship between metabolites/lipids and community composition following *Salmonella* infection. We found 157 pairs of positively linked metabolites/lipids and gut bacteria (correlation coefficient > 0.7, p-value < 0.05) and 596 pairs of negatively correlated metabolites/lipids and gut microbes (correlation coefficient < -0.7, p-value < 0.05). Positively correlated pairs (lipids/metabolites and microorganisms) include a correlation between glycerolipids and the class of *Clostridia*. In detail, metabolites/lipids such as monogalactosyldiacylglycerol (MGDG) and oxidized MGDG were positively correlated with the

*Lachnospiraceae* and *Roseburia* genera. MGDG and oxidized MGDG were positively correlated with the *Bacteroidia* class including the *Muribaculaceae* genus. The observed connections suggest a potential involvement of gut bacteria in the metabolic pathways of the linked metabolites/lipids, or a possible source of the substances. According to reports, MGDGs are widely dispersed in the *Clostridia* class<sup>39,40</sup> (Figure S2). In addition, correlation analysis was performed at each time point of *Salmonella* infection. Only 25 correlation pairs (7 positive correlation pairs and 18 negative correlation pairs) were observed at the early time point of *Salmonella* infection, but 682 correlation pairs (273 positive correlation pairs and 409 negative correlation pairs) and 3864 correlation pairs (755 positive correlation pairs and 3109 negative correlation pairs), respectively, were observed at the mid and late time points of *Salmonella* infection (Figure S2). More correlation was observed at the late time point of *Salmonella* infection, as there were more dramatic changes in gut microbial composition and in abundances of metabolites/lipids. Figure 5 illustrates a network analysis of the fifteen metabolites/lipids most highly correlated with *Salmonella*. Esterified deoxycholic acids, such as sterol ester (SE) 24:1;O4/18:0;O and SE 24:1;O4/16:0;O, were negatively correlated with *Salmonella*, but many glycerophospholipids, including glycerophosphatidylethanolamines, were positively correlated. As discussed previously, dysbiosis caused by *Salmonella* infection reduced or deactivated the microbial bile acid metabolism. The negative connection between esterified deoxycholic acids and *Salmonella* provides evidence for a decreased amount of esterified deoxycholic acids as result of *Salmonella* infection.

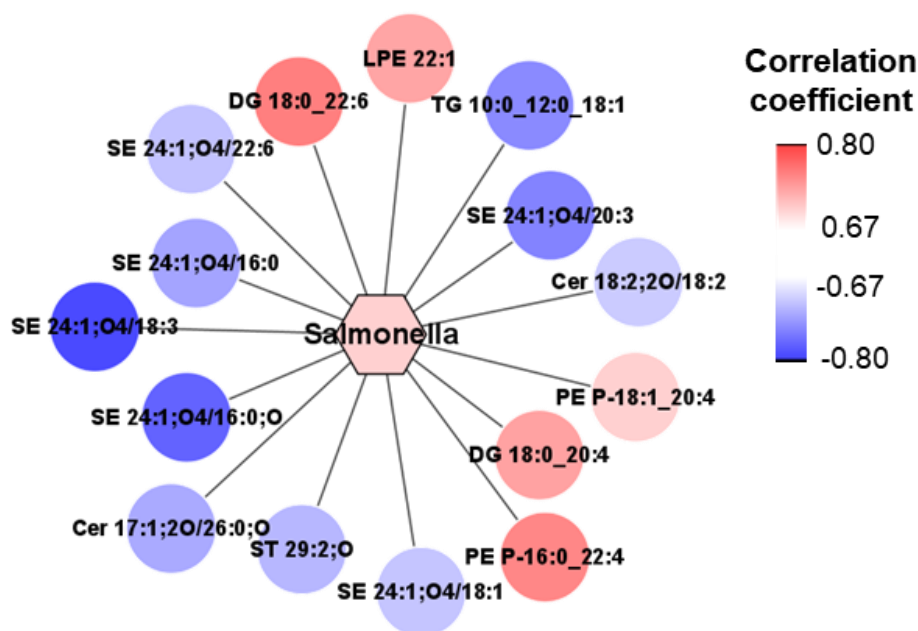


**Figure 5.** Top 15 metabolites/lipids correlated to *Salmonella* bacteria were extracted from Figure S2.

### Integration of meta-transcriptomics and metabolomics/lipidomics to investigate the impact of dysbiosis induced by *Salmonella* infection at the late time point

As indicated in the above paragraph, significant metabolome/lipidome changes were identified between HR and LR mice. Changes in the composition of intestinal microbes as determined by 16s rRNA indicated that HR mice had a more severe *dysbiosis*. We conducted a meta-transcriptomics analysis that provides the expression profiles of microbial communities and *Salmonella* to examine the effect of gut microbial alteration on metabolic pathways that are significantly distinct between HR and LR groups. Figure 6 illustrates the relationship between metabolomics/lipidomics driven metabolic pathways and the expressed microbial metabolic pathways that are involved in those metabolic pathways. ((A): amino acids, (B): lipids, (C) energy and carbohydrate, and (D) other metabolisms) These global perspectives on metabolic pathways

assisted the identification of the key contributing taxa of metabolic pathways in each group. For instance, *Bacteroidia* contribute the most to amino acid metabolism, including cysteine and methionine metabolism, histidine metabolism, and lysine degradation, in the LR group, whereas *Gammaproteobacteria* are the most important contributors in the HR group. *Bacilli* belonging to the HR group are actively involved in lysine degradation and tryptophan metabolism, whilst *Bacilli* belonging to the LR group are also strongly involved in arginine biosynthesis and arginine and proline metabolism. *Bacilli* class encompasses five distinct families: *Anaeroplasmataceae*, *Erysipelatoclostridiaceae*, *Enterococcaceae*, *Lactobacillaceae*, and *Erysipelotrichaceae*. Highly expressed *Bacilli* class genes in the HR mice were from the family *Enterococcoace* which co-enriched with *Salmonella*, but highly expressed *Bacilli* class genes in the LR mice were from families other than *Enterococcoace*. Based on the results of metabolomics/lipidomics, four lipid metabolisms (glycerolipid metabolism, glycerophospholipid metabolism, ether lipid metabolism, and primary bile acid metabolism) were significantly different between HR and LR mice, and gut bacteria participated in those metabolic pathways. As shown, the *Gammaproteobacteria* genes involved in glycerophospholipid metabolism, glycerolipid metabolism, and ether lipid metabolism are substantially expressed in HR mice relative to LR mice. *Clostridia* and *Bacilli* classes have been found to be associated with primary bile acid metabolism, however the level of correlation seen here was not substantial. We concluded that the direct influence of the gut microbiota on primary bile acid metabolism is modest as mice are predominantly in charge of primary bile acid metabolism.<sup>41</sup> On the other hand, secondary bile acid metabolism is strongly associated with six gut microbes (families *Lachnospiraceae*, *Ruminococcaceae*, *Erysipelatoclostridiaceae*, *Oscillospiraceae*, *Acutalibacteraceae*, and *Lactobacillaceae*) and can influence the enterohepatic cycling of bile acids, thereby influencing the primary bile acid metabolism of the host.<sup>26</sup>

Metabolism of secondary bile acids is disturbed in HR mice, as evidenced by the lower quantity of secondary bile acids detected by metabolomics/lipidomics. The interruption of the secondary bile acid metabolism can impair the primary bile acid metabolism of the host.

In Figure 7, we illustrate *Salmonella* functional profile differences between HR and LR mice at the late time point of infection. We discovered distinctive active *Salmonella* metabolisms in the HR group, which include sulfur metabolism and reductases and an electron transport chain component, and the genes involved in these two metabolic pathways were only expressed in *Salmonella*. *Salmonella* bacteria utilize sulfur metabolism for their multiplication and competition with other intestinal microorganisms.<sup>42</sup> The reactive oxygen species created during inflammation can react with luminal sulfur compounds such as thiosulfate, and as a result, they can be transformed into tetrathionate, which serves as a *Salmonella* respiratory electron acceptor.<sup>42</sup> *Salmonella* can utilize carbon sources from the host, such as ethanolamine, via tetrathionate respiration during anaerobic respiration.<sup>42-44</sup>

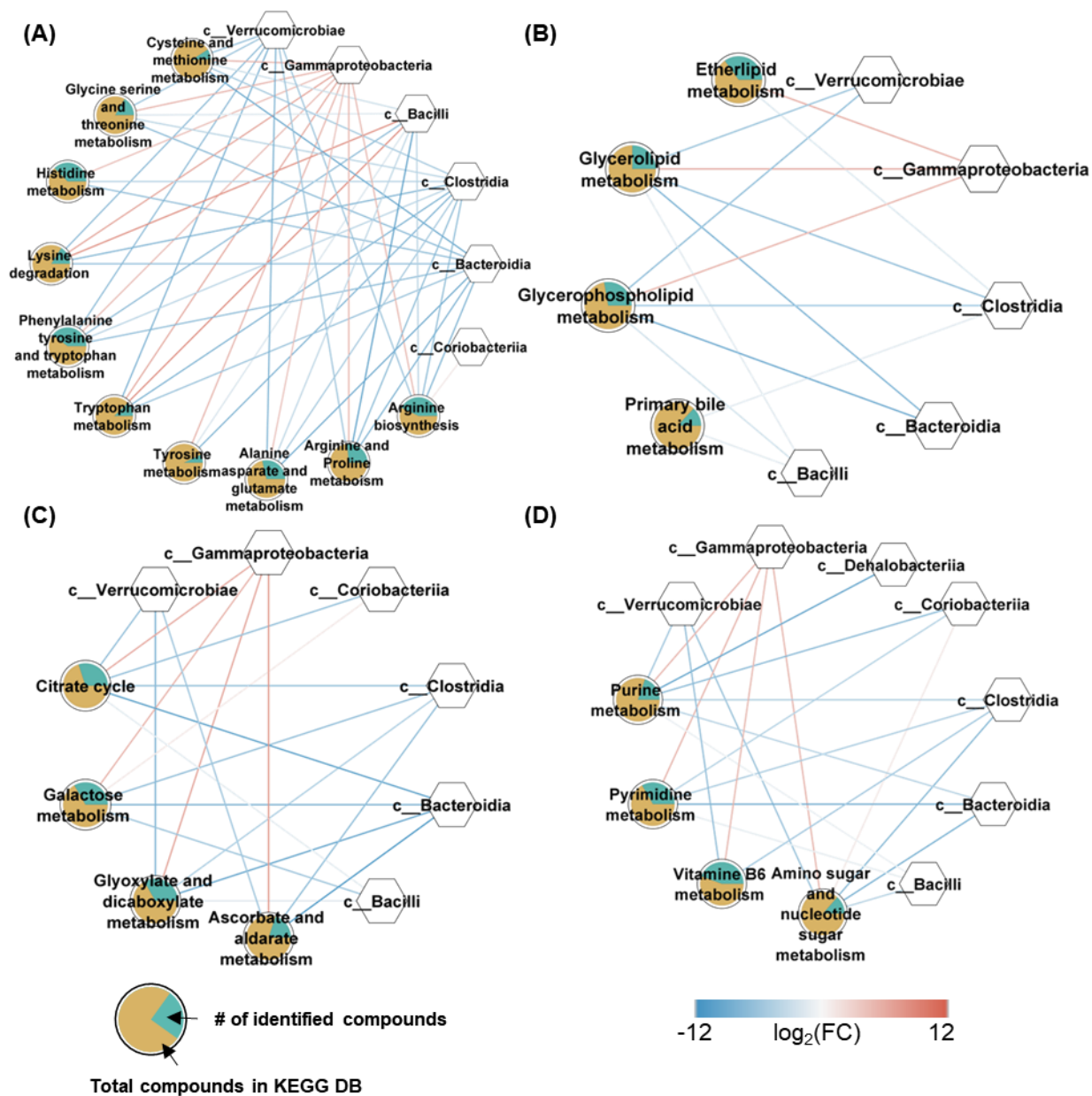


**Figure 6.** Relationships between gut microbial taxa and metabolomics/lipidomics driven metabolic pathways ((A): amino acids, (B): lipids, (C) energy and carbohydrate, and (D) other metabolisms). The line color represents the  $\log_2(\text{fold change} = \text{abundance in HR}/\text{abundance in LR})$

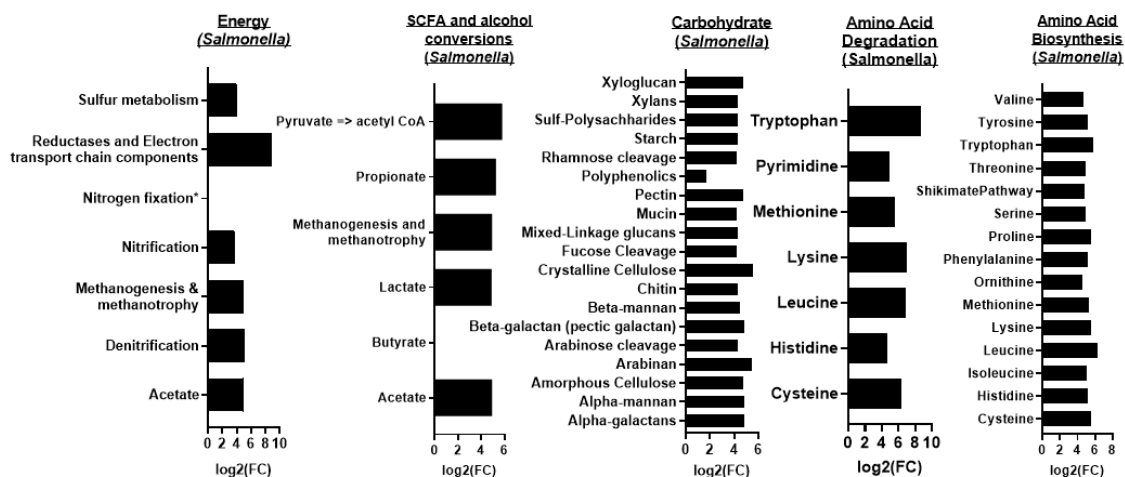
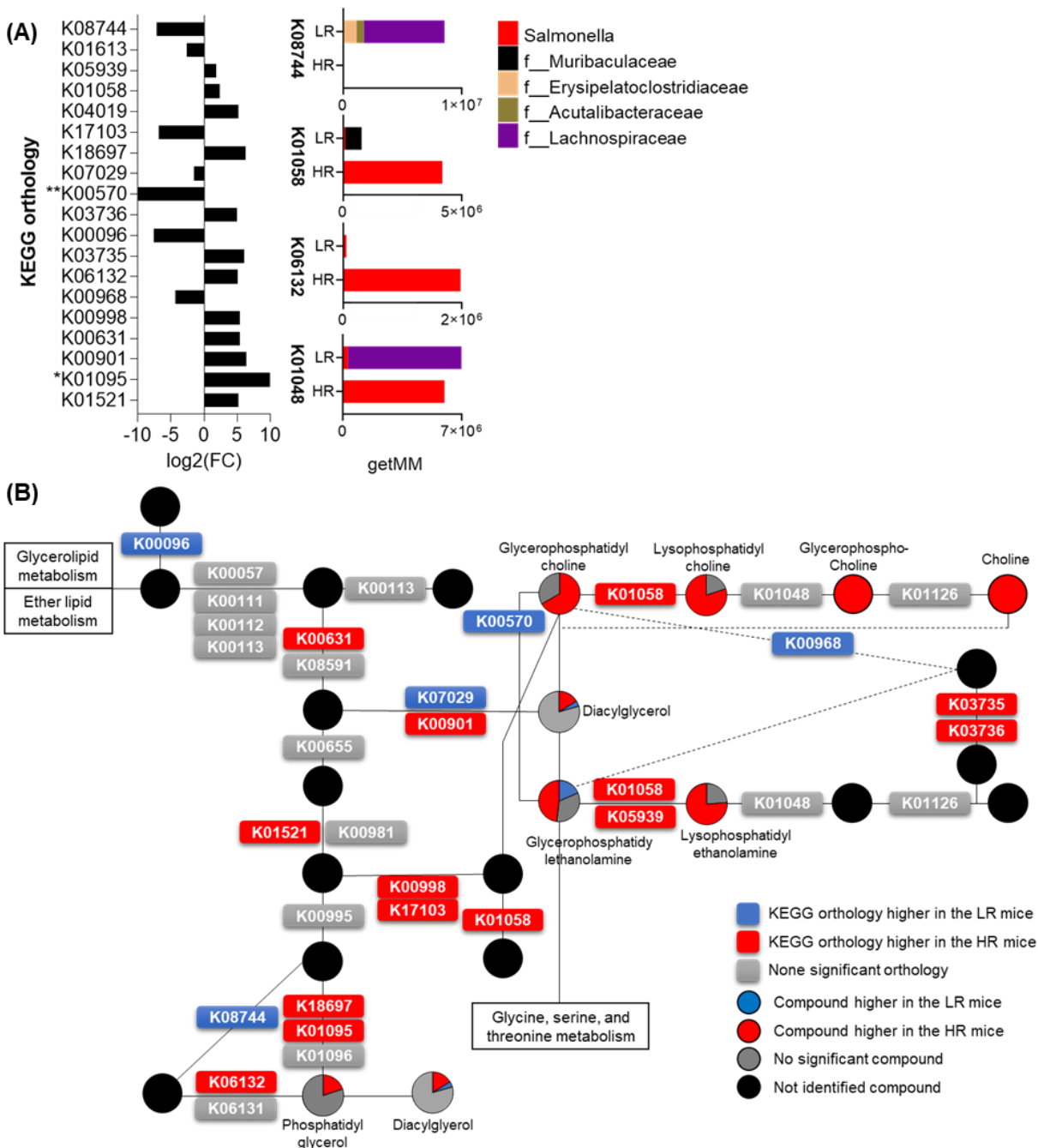


**Figure 7.** Transcriptome based *Salmonella* metabolism. Fold change was calculated by abundance in HR group divided by abundance in LR group.

We studied further the effect of gut microbes and *Salmonella* infection on the key pathways identified by metabolomics/lipidomics data. There are a total of 19 KEGG orthologies (KOs) involved in glycerophospholipid metabolism, as shown in Figure 8A. Thirty-three species of microorganisms belonging to 9 families expressed the genes involved in KOs. In LR mice, twelve KOs, including K06142 and K01058, were highly active. In HR mice, K06132 (cardiolipin synthase C) and K01058 (Phospholipase A1/A2) were exclusively expressed from *Salmonella*; in LR mice, however, they were also expressed by the *Muribaculaceae* family and *Salmonella*. Compared to HR mice, the total number of expressed genes was significantly lower in LR mice. Seven KOs exhibited decreased abundance in HR mice, including K08744 (cardiolipin synthase (CMP-forming)). K01048 (lysophospholipase), an enzyme that releases fatty acids from lysophospholipids, had an insignificant FC difference for HR vs. LR mice. However, the gut microorganisms that expressed K01048 were dissimilar. *Salmonella* dominated the release of K01048 in the HR group, whereas the *Lachnospiraceae* family was a significant contributor in the LR group. Mapping the identified metabolites/lipids offers a better understanding of changed

pathways; hence, we mapped 196 unique lipids and metabolites classified into the eight KEGG IDs implicated in glycerophospholipid metabolism (Figure 8B). The significantly stimulated metabolic flux of PC and PE in HR mice is one of the most intriguing aspects of this figure. Due to the increased number of dead epithelial cells caused by the host inflammatory response, PC and PE levels are elevated in an inflamed gut environment. In LR mice, the gut microbial functions implicated in the glycerophospholipid production pathway, such as K00570 (phosphatidylethanolamine/phosphatidyl-N-methylethanolamine N-methyltransferase) and K00968 (choline-phosphate cytidyltransferase), were significantly active. However, lipidomics demonstrated that over 66 percent of identified PCs (28/42, numbers of significant PCs / numbers of identified PCs) had a considerably higher abundance in the HR group, but none of them were significantly more abundant in the LR group. This suggests that the greater abundance of PCs in the HR group is a result of the host immune response and not the gut microbiome. The majority of LPCs (16/20) were likewise greater in the HR groups, however no LPCs of significance were identified in the LR group. *Salmonella* bacteria can use these increased glycerophospholipids. In HR mice, *Salmonella* phospholipases A1/A2 (K01058 and K05939) that convert PCs (or PEs) into LPCs (or LPEs) were expressed at a higher level. *Salmonella's* active PC digesting metabolism results in the buildup of glycerophosphocholine and choline. Ethanolamine, which is produced after PE digestion and utilized by bacterial pathogens such as *Salmonella*, was not identified in this study; however, we observed a greater abundance of genes involved in ethanolamine **consumption** by *Salmonella*, including K03735 (ethanolamine ammonia-lyase large subunit) and K03736 (ethanolamine ammonia-lyase small subunit). Choline and ethanolamine are both carbon and energy sources for *Salmonella* development in the intestine.<sup>45</sup>



Another example of a key pathway that revealed the difference between the HR and LR groups at the late time point is the tryptophan metabolism pathway. (Figure 9) Tryptophan is a precursor molecule of indole, and indole is metabolized by gut microorganisms. One of the metabolic pathways that we observed was tryptophan transformation, where tryptophan is converted into indole derivatives such as indole-acetate and 2-oxoindole-3-acetate in the LR mice. Indole-acetate can bind to the aryl hydrocarbon receptor (AhR), which lowers pro-inflammatory cytokine expression and regulates the formation of intraepithelial lymphocytes, which play a crucial role in pathogen invasion defense.<sup>46,47</sup> Presumably, the increased quantity of indole-acetate in the LR mice inhibits *Salmonella* development, promotes gut microbial balance, and prevents dysbiosis from occurring. However, further study is needed to prove this. In contrast, we detected a significantly elevated level of tryptophan in the HR group. We concluded that the tryptophan was deposited due to the gut microbial community of HR mice lacking the capacity to generate anti-inflammatory indole derivatives. *Salmonella* increased expression of K01825 (3-hydroxyacyl-CoA dehydrogenase / enoyl-CoA hydratase / 3-hydroxybutyryl-CoA epimerase / enoyl-CoA isomerase), K01782 (3-hydroxyacyl-CoA dehydrogenase / enoyl-CoA hydratase / 3-hydroxybutyryl-CoA epimerase/ enoyl-CoA isomerase) and K01782 (3-hydroxyacyl-CoA dehydrogenase / enoyl-CoA hydratase / 3-hydroxybutyryl-CoA epimerase). Expression in these pathways by *Salmonella* implies that the accumulated tryptophan in the HR group is catabolized and converted to acetyl-CoA to be used for glycolysis.

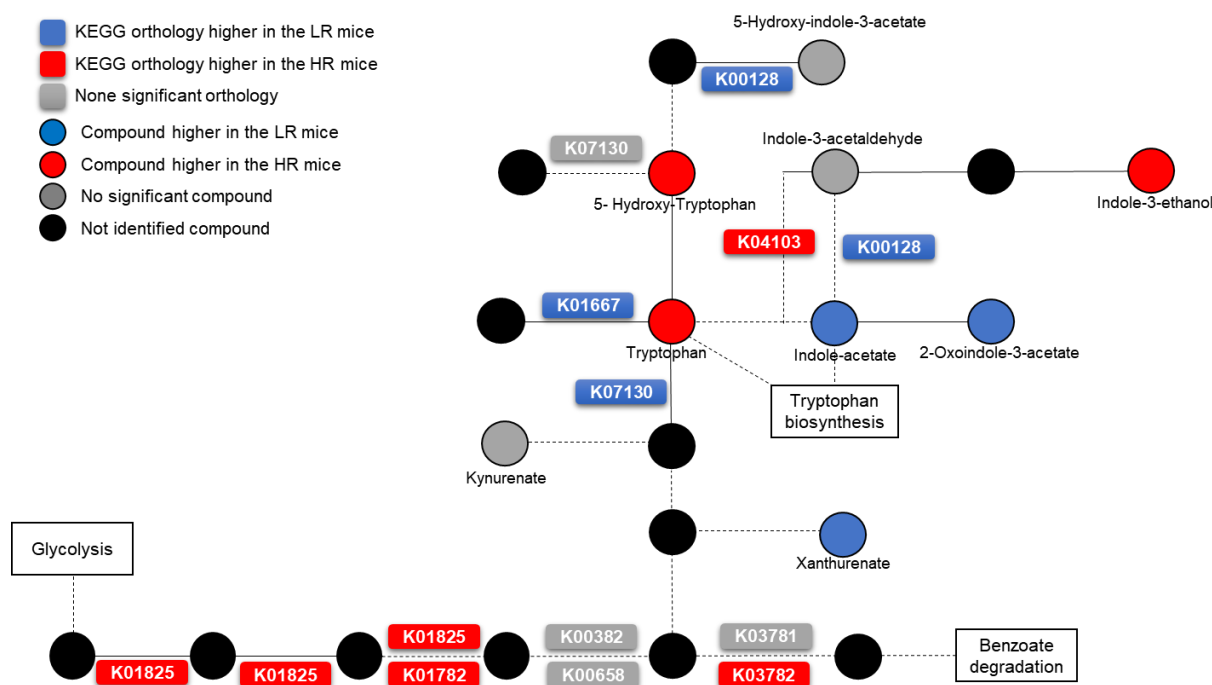


**Figure 9.** KEGG tryptophan metabolism mapped with the meta-transcriptomics and metabolomics/results.

## Conclusions

In summary, this work highlights the different metabolic changes of *Salmonella* infected mice according to infection phase. Multiple metabolic pathways were affected at each investigated time point. Integrated multi-omics analysis with 16S rRNA sequencing and metatranscriptomics implied that many host metabolism changes after *Salmonella* infections were induced by dysbiosis. Some of the altered metabolic pathways, such as bile acid metabolism, tryptophan metabolism, and glycerophospholipid metabolism, demonstrated congruence with results reported in other studies, where gut microbiome composition was altered for various reasons.<sup>32,48–50</sup> Although cholesterol esterification was not extensively researched in previous *Salmonella* studies, our findings indicate that cholesterol esterification levels rose during *Salmonella* infection, likely because of ceramide accumulation. At the late time point, there were distinctive metabolite and

lipid patterns between high and low responders, indicating the influence of *Salmonella* abundance on the gut environment and host metabolism. For example, the gut microbiota can metabolize tryptophan to produce indole-acetate and 2-oxoindole-3-acetate when the *Salmonella* abundance is low. *Salmonella* can, however, accumulate and use tryptophan for glycolysis in an intestinal environment where they are the dominant bacteria. In *Salmonella*-dominant environments, *Salmonella* utilizes glycerophosphocholines and glycerophosphoethanolamines, produced by the host's inflammatory response, as carbon and energy sources for growth. Based on our findings, further investigation can be undertaken to examine the roles of various lipids and metabolites, especially microbial driven metabolites such as indole derivatives against various pathogenic invasion. These findings hold promise for the contribution to the development of therapeutic treatments and the discovery and advancement of drugs.

## **ASSOCIATED CONTENT**

### **Supporting Information**

Statistical results for identified metabolites/lipids (Table S1); Metabolomics/lipidomics driven pathway analysis result (Table S2); Correlation analysis between metabolomics/lipidomics and 16s rRNA analysis (Table S3); Meta-transcriptomics analysis result (Table S4); The abundance of *Salmonella* of 40 mice (Figure S1); Correlation analysis between 16s rRNA result and metabolomics/lipidomics result at each time point of *Salmonella* infection. Correlation result (Figure S2).

## **AUTHOR INFORMATION**

## **Corresponding Author**

Vicki H. Wysocki – Department of Chemistry and Biochemistry and Native Mass Spectrometry Guided Structural Biology Center, The Ohio State University, Columbus, Ohio, 43210, United States; [orcid.org/0000-0003-0495-2538](https://orcid.org/0000-0003-0495-2538); [wysocki.11@osu.edu](mailto:wysocki.11@osu.edu)

## **Present Addresses**

Yongseok Kim – Department of Chemistry and Biochemistry, The Ohio State University, Columbus, Ohio, 43210, United States; [orcid.org/0000-0001-7861-7375](https://orcid.org/0000-0001-7861-7375); [kim.7263@osu.edu](mailto:kim.7263@osu.edu)

Katherine Kokkinias – Department of Microbiology, Immunology, and Pathology, Colorado State University, Fort Collins, Colorado, 80523, United States; [Katherine.Kokkinias@colostate.edu](mailto:Katherine.Kokkinias@colostate.edu)

Anice Sabag-Daigle – Department of Microbiology, The Ohio State University, Columbus, Ohio, 43210, United States; [sabag-daigle.1@osu.edu](mailto:sabag-daigle.1@osu.edu)

Ikaia Lelewi – Department of Cell & Molecular Biology, Colorado State University, Fort Collins, Colorado, 80523, United States; [orcid.org/0000-0002-9200-6340](https://orcid.org/0000-0002-9200-6340); [ikaia.lelewi@colostate.edu](mailto:ikaia.lelewi@colostate.edu)

Mikayla Borton – Department of Soil and Crop Sciences, Colorado State University, Fort Collins, Colorado, 80523, United States; [Mikayla.Borton@colostate.edu](mailto:Mikayla.Borton@colostate.edu)

Michael Shaffer – Department of Soil and Crop Sciences, Colorado State University, Fort Collins, Colorado, 80523, United States; [michael.t.shaffer@colostate.edu](mailto:michael.t.shaffer@colostate.edu)

Maryam Baniasad – Department of Chemistry and Biochemistry, The Ohio State University, Columbus, Ohio, 43210, United States; [baniasad.1@osu.edu](mailto:baniasad.1@osu.edu)

Rebecca Daly – Department of Soil and Crop Sciences, Colorado State University, Fort Collins, Colorado, 80523, United States; Reb.Daly@colostate.edu

Brian M.M. Ahmer –Department of Microbiology, The Ohio State University, Columbus, Ohio, 43210, United States; ahmer.1@osu.edu

Kelly C. Wrighton – Department of Soil and Crop Sciences, Colorado State University, Fort Collins, Colorado, 80523 United States; Kelly.Wrighton@colostate.edu

### **Author Contributions**

All authors were involved in the planning and refinement of the experimental approach and discussed the data and the multiple data types. Y.K. wrote the first and revised draft of the manuscript and all authors contributed to writing and revising the manuscript. Y.K. and M.B. (Maryam Baniasad) contributed to data collection and analysis of MS based metabolomics and lipidomics. K.K., I.K., M.B. (Mikayla Borton), M.S., R.B and K.W. conducted data collection and interpretation of 16s rRNA sequencing and metatranscriptomics. A.S. and B.A. led the mouse study and sample collection. V.W. provided scientific direction, revised the paper extensively, and supervised the entire study. All authors have given approval to the final version of the manuscript.

### **Funding Sources**

This work was supported by the grant number 5R01AI43288 from the National Institutes of Health (NIH). LC-MS/MS access was provided by the OSU NIH P30CA016058 CCC Proteomics Shared Resource embedded in the OSU Campus Chemical Instrument Center.

### **ACKNOWLEDGMENT**

The authors thank the OSU Campus Chemical Instrument Center – Mass spectrometry & Proteomics facility and the Ohio State University Comprehensive Cancer Center (OSU CCC) for helping us use and operate the LC-MS/MS instrument.

## REFERENCES

- (1) Giannella, R. A. Salmonella. In *Medical Microbiology*; Baron, S., Ed.; University of Texas Medical Branch at Galveston: Galveston (TX), 1996.
- (2) Galán, J. E. Salmonella Typhimurium and Inflammation: A Pathogen-Centric Affair. *Nat Rev Microbiol* **2021**, *19* (11), 716–725. <https://doi.org/10.1038/s41579-021-00561-4>.
- (3) Borton, M. A.; Sabag-Daigle, A.; Wu, J.; Solden, L. M.; O'Banion, B. S.; Daly, R. A.; Wolfe, R. A.; Gonzalez, J. F.; Wysocki, V. H.; Ahmer, B. M. M.; Wrighton, K. C. Chemical and Pathogen-Induced Inflammation Disrupt the Murine Intestinal Microbiome. *Microbiome* **2017**, *5* (1), 47. <https://doi.org/10.1186/s40168-017-0264-8>.
- (4) Stecher, B.; Robbiani, R.; Walker, A. W.; Westendorf, A. M.; Barthel, M.; Kremer, M.; Chaffron, S.; Macpherson, A. J.; Buer, J.; Parkhill, J.; Dougan, G.; Mering, C. von; Hardt, W.-D. Salmonella Enterica Serovar Typhimurium Exploits Inflammation to Compete with the Intestinal Microbiota. *PLOS Biology* **2007**, *5* (10), e244. <https://doi.org/10.1371/journal.pbio.0050244>.
- (5) Gillis, C. C.; Hughes, E. R.; Spiga, L.; Winter, M. G.; Zhu, W.; Furtado de Carvalho, T.; Chanin, R. B.; Behrendt, C. L.; Hooper, L. V.; Santos, R. L.; Winter, S. E. Dysbiosis-Associated Change in Host Metabolism Generates Lactate to Support Salmonella Growth. *Cell Host & Microbe* **2018**, *23* (1), 54-64.e6. <https://doi.org/10.1016/j.chom.2017.11.006>.
- (6) Rogers, A. W. L.; Tsolis, R. M.; Bäuml, A. J. Salmonella versus the Microbiome. *Microbiology and Molecular Biology Reviews* **85** (1), e00027-19. <https://doi.org/10.1128/MMBR.00027-19>.
- (7) L, M.; Mj, B.; M, Ú.; E, C.; R, D. C.; M, R.-S.; M, L.; Am, S.-D.; O, P.; D, D.; L, G.-B.; J, M.; M, Á.-M.; A, A. Intestinal Immune Dysregulation Driven by Dysbiosis Promotes Barrier Disruption and Bacterial Translocation in Rats With Cirrhosis. *Hepatology (Baltimore, Md.)* **2019**, *70* (3). <https://doi.org/10.1002/hep.30349>.
- (8) Yoo, J. Y.; Groer, M.; Dutra, S. V. O.; Sarkar, A.; McSkimming, D. I. Gut Microbiota and Immune System Interactions. *Microorganisms* **2020**, *8* (10), 1587. <https://doi.org/10.3390/microorganisms8101587>.
- (9) Kurtz, J. R.; Goggins, J. A.; McLachlan, J. B. Salmonella Infection: Interplay between the Bacteria and Host Immune System. *Immunology Letters* **2017**, *190*, 42–50. <https://doi.org/10.1016/j.imlet.2017.07.006>.
- (10) Zeng, M. Y.; Inohara, N.; Nuñez, G. Mechanisms of Inflammation-Driven Bacterial Dysbiosis in the Gut. *Mucosal Immunol* **2017**, *10* (1), 18–26. <https://doi.org/10.1038/mi.2016.75>.
- (11) Tsugawa, H.; Ikeda, K.; Takahashi, M.; Satoh, A.; Mori, Y.; Uchino, H.; Okahashi, N.; Yamada, Y.; Tada, I.; Bonini, P.; Higashi, Y.; Okazaki, Y.; Zhou, Z.; Zhu, Z.-J.; Koelmel, J.;

- Cajka, T.; Fiehn, O.; Saito, K.; Arita, M.; Arita, M. A Lipidome Atlas in MS-DIAL 4. *Nat Biotechnol* **2020**, *38* (10), 1159–1163. <https://doi.org/10.1038/s41587-020-0531-2>.
- (12) Fahy, E.; Subramaniam, S.; Murphy, R. C.; Nishijima, M.; Raetz, C. R. H.; Shimizu, T.; Spener, F.; van Meer, G.; Wakelam, M. J. O.; Dennis, E. A. Update of the LIPID MAPS Comprehensive Classification System for Lipids. *J Lipid Res* **2009**, *50* (Suppl), S9–S14. <https://doi.org/10.1194/jlr.R800095-JLR200>.
- (13) Pang, Z.; Zhou, G.; Ewald, J.; Chang, L.; Hacariz, O.; Basu, N.; Xia, J. Using MetaboAnalyst 5.0 for LC–HRMS Spectra Processing, Multi-Omics Integration and Covariate Adjustment of Global Metabolomics Data. *Nat Protoc* **2022**, *17* (8), 1735–1761. <https://doi.org/10.1038/s41596-022-00710-w>.
- (14) Xiao, H.-H.; Sham, T.-T.; Chan, C.-O.; Li, M.-H.; Chen, X.; Wu, Q.-C.; Mok, D. K.-W.; Yao, X.-S.; Wong, M.-S. A Metabolomics Study on the Bone Protective Effects of a Lignan-Rich Fraction From *Sambucus Williamsii* Ramulus in Aged Rats. *Front Pharmacol* **2018**, *9*, 932. <https://doi.org/10.3389/fphar.2018.00932>.
- (15) Caporaso, J. G.; Lauber, C. L.; Walters, W. A.; Berg-Lyons, D.; Lozupone, C. A.; Turnbaugh, P. J.; Fierer, N.; Knight, R. Global Patterns of 16S rRNA Diversity at a Depth of Millions of Sequences per Sample. *Proceedings of the National Academy of Sciences* **2011**, *108* (supplement\_1), 4516–4522. <https://doi.org/10.1073/pnas.1000080107>.
- (16) Bolyen, E.; Rideout, J. R.; Dillon, M. R.; Bokulich, N. A.; Abnet, C. C.; Al-Ghalith, G. A.; Alexander, H.; Alm, E. J.; Arumugam, M.; Asnicar, F.; Bai, Y.; Bisanz, J. E.; Bittinger, K.; Brejnrod, A.; Brislawn, C. J.; Brown, C. T.; Callahan, B. J.; Caraballo-Rodríguez, A. M.; Chase, J.; Cope, E. K.; Da Silva, R.; Diener, C.; Dorrestein, P. C.; Douglas, G. M.; Durall, D. M.; Duvallet, C.; Edwardson, C. F.; Ernst, M.; Estaki, M.; Fouquier, J.; Gauglitz, J. M.; Gibbons, S. M.; Gibson, D. L.; Gonzalez, A.; Gorlick, K.; Guo, J.; Hillmann, B.; Holmes, S.; Holste, H.; Huttenhower, C.; Huttley, G. A.; Janssen, S.; Jarmusch, A. K.; Jiang, L.; Kaehler, B. D.; Kang, K. B.; Keefe, C. R.; Keim, P.; Kelley, S. T.; Knights, D.; Koester, I.; Kosciulek, T.; Kreps, J.; Langille, M. G. I.; Lee, J.; Ley, R.; Liu, Y.-X.; Lofffield, E.; Lozupone, C.; Maher, M.; Marotz, C.; Martin, B. D.; McDonald, D.; McIver, L. J.; Melnik, A. V.; Metcalf, J. L.; Morgan, S. C.; Morton, J. T.; Naimey, A. T.; Navas-Molina, J. A.; Nothias, L. F.; Orchanian, S. B.; Pearson, T.; Peoples, S. L.; Petras, D.; Preuss, M. L.; Pruesse, E.; Rasmussen, L. B.; Rivers, A.; Robeson, M. S.; Rosenthal, P.; Segata, N.; Shaffer, M.; Shiffer, A.; Sinha, R.; Song, S. J.; Spear, J. R.; Swafford, A. D.; Thompson, L. R.; Torres, P. J.; Trinh, P.; Tripathi, A.; Turnbaugh, P. J.; Ul-Hasan, S.; van der Hooft, J. J. J.; Vargas, F.; Vázquez-Baeza, Y.; Vogtmann, E.; von Hippel, M.; Walters, W.; Wan, Y.; Wang, M.; Warren, J.; Weber, K. C.; Williamson, C. H. D.; Willis, A. D.; Xu, Z. Z.; Zaneveld, J. R.; Zhang, Y.; Zhu, Q.; Knight, R.; Caporaso, J. G. Reproducible, Interactive, Scalable and Extensible Microbiome Data Science Using QIIME 2. *Nat Biotechnol* **2019**, *37* (8), 852–857. <https://doi.org/10.1038/s41587-019-0209-9>.
- (17) Quast, C.; Pruesse, E.; Yilmaz, P.; Gerken, J.; Schweer, T.; Yarza, P.; Peplies, J.; Glöckner, F. O. The SILVA Ribosomal RNA Gene Database Project: Improved Data Processing and Web-Based Tools. *Nucleic Acids Res* **2013**, *41* (Database issue), D590–D596. <https://doi.org/10.1093/nar/gks1219>.
- (18) Quinn, T. P.; Erb, I. Examining Microbe–Metabolite Correlations by Linear Methods. *Nat Methods* **2021**, *18* (1), 37–39. <https://doi.org/10.1038/s41592-020-01006-1>.
- (19) Lelewi, I.; Rodriguez-Ramos, J.; Shaffer, M.; Sabag-Daigle, A.; Kokkinias, K.; Flynn, R. M.; Daly, R. A.; Kop, L. F.; Solden, L. M.; Ahmer, B. M. M.; Borton, M. A.; Wrighton, K.

- C. Exposing New Taxonomic Variation with Inflammation – A Murine Model-Specific Genome Database for Gut Microbiome Researchers. *bioRxiv* October 24, 2022, p 2022.10.24.513540. <https://doi.org/10.1101/2022.10.24.513540>.
- (20) Langmead, B.; Salzberg, S. L. Fast Gapped-Read Alignment with Bowtie 2. *Nat Methods* **2012**, *9* (4), 357–359. <https://doi.org/10.1038/nmeth.1923>.
- (21) Anders, S.; Pyl, P. T.; Huber, W. HTSeq—a Python Framework to Work with High-Throughput Sequencing Data. *Bioinformatics* **2015**, *31* (2), 166–169. <https://doi.org/10.1093/bioinformatics/btu638>.
- (22) Love, M. I.; Huber, W.; Anders, S. Moderated Estimation of Fold Change and Dispersion for RNA-Seq Data with DESeq2. *Genome Biology* **2014**, *15* (12), 550. <https://doi.org/10.1186/s13059-014-0550-8>.
- (23) Smid, M.; Coebergh van den Braak, R. R. J.; van de Werken, H. J. G.; van Riet, J.; van Galen, A.; de Weerd, V.; van der Vlugt-Daane, M.; Bril, S. I.; Lalmahomed, Z. S.; Kloosterman, W. P.; Wilting, S. M.; Foekens, J. A.; IJzermans, J. N. M.; Coene, P. P. L. O.; Dekker, J. W. T.; Zimmerman, D. D. E.; Tetteroo, G. W. M.; Vles, W. J.; Vrijland, W. W.; Torenbeek, R.; Kliffen, M.; Carel Meijer, J. H.; vd Wurff, A. A.; Martens, J. W. M.; Sieuwerts, A. M.; on behalf of the MATCH study group. Gene Length Corrected Trimmed Mean of M-Values (GeTMM) Processing of RNA-Seq Data Performs Similarly in Intersample Analyses While Improving Intrasample Comparisons. *BMC Bioinformatics* **2018**, *19* (1), 236. <https://doi.org/10.1186/s12859-018-2246-7>.
- (24) Sun, M.; Du, B.; Shi, Y.; Lu, Y.; Zhou, Y.; Liu, B. Combined Signature of the Fecal Microbiome and Plasma Metabolome in Patients with Ulcerative Colitis. *Med Sci Monit* **2019**, *25*, 3303–3315. <https://doi.org/10.12659/MSM.916009>.
- (25) Liu, Y.; Zhang, S.; Zhou, W.; Hu, D.; Xu, H.; Ji, G. Secondary Bile Acids and Tumorigenesis in Colorectal Cancer. *Frontiers in Oncology* **2022**, *12*.
- (26) Hofmann, A. F. The Continuing Importance of Bile Acids in Liver and Intestinal Disease. *Archives of Internal Medicine* **1999**, *159* (22), 2647–2658. <https://doi.org/10.1001/archinte.159.22.2647>.
- (27) Guzior, D. V.; Quinn, R. A. Review: Microbial Transformations of Human Bile Acids. *Microbiome* **2021**, *9* (1), 140. <https://doi.org/10.1186/s40168-021-01101-1>.
- (28) Alegado, R. A.; Brown, L. W.; Cao, S.; Dermenjian, R. K.; Zuzow, R.; Fairclough, S. R.; Clardy, J.; King, N. A Bacterial Sulfonolipid Triggers Multicellular Development in the Closest Living Relatives of Animals. *eLife* **2012**, *1*, e00013. <https://doi.org/10.7554/eLife.00013>.
- (29) Walker, A.; Pfitzner, B.; Harir, M.; Schaubeck, M.; Calasan, J.; Heinzmann, S. S.; Turaev, D.; Rattei, T.; Endesfelder, D.; Castell, W. zu; Haller, D.; Schmid, M.; Hartmann, A.; Schmitt-Kopplin, P. Sulfonolipids as Novel Metabolite Markers of *Alistipes* and *Odoribacter* Affected by High-Fat Diets. *Sci Rep* **2017**, *7* (1), 11047. <https://doi.org/10.1038/s41598-017-10369-z>.
- (30) Lynch, A.; Crowley, E.; Casey, E.; Cano, R.; Shanahan, R.; McGlacken, G.; Marchesi, J. R.; Clarke, D. J. The Bacteroidales Produce an N-Acylated Derivative of Glycine with Both Cholesterol-Solubilising and Hemolytic Activity. *Sci Rep* **2017**, *7* (1), 13270. <https://doi.org/10.1038/s41598-017-13774-6>.
- (31) Kriaa, A.; Bourgin, M.; Potiron, A.; Mkaouar, H.; Jablaoui, A.; Gérard, P.; Maguin, E.; Rhimi, M. Microbial Impact on Cholesterol and Bile Acid Metabolism: Current Status and

- Future Prospects. *Journal of Lipid Research* **2019**, *60* (2), 323–332. <https://doi.org/10.1194/jlr.R088989>.
- (32) Zhu, Y.; Gu, L.; Lin, X.; Zhang, J.; Tang, Y.; Zhou, X.; Lu, B.; Lin, X.; Liu, C.; Prochownik, E. V.; Li, Y. Ceramide-Mediated Gut Dysbiosis Enhances Cholesterol Esterification and Promotes Colorectal Tumorigenesis in Mice. *JCI Insight* **2022**, *7* (3). <https://doi.org/10.1172/jci.insight.150607>.
- (33) Lordan, R.; Tsoupras, A.; Zabetakis, I. Phospholipids of Animal and Marine Origin: Structure, Function, and Anti-Inflammatory Properties. *Molecules* **2017**, *22* (11), E1964. <https://doi.org/10.3390/molecules22111964>.
- (34) Treede, I.; Braun, A.; Sparla, R.; Kühnel, M.; Giese, T.; Turner, J. R.; Anes, E.; Kulaksiz, H.; Füllekrug, J.; Stremmel, W.; Griffiths, G.; Ehehalt, R. Anti-Inflammatory Effects of Phosphatidylcholine. *J Biol Chem* **2007**, *282* (37), 27155–27164. <https://doi.org/10.1074/jbc.M704408200>.
- (35) Chen, M.; Pan, H.; Dai, Y.; Zhang, J.; Tong, Y.; Huang, Y.; Wang, M.; Huang, H. Phosphatidylcholine Regulates NF- $\kappa$ B Activation in Attenuation of LPS-Induced Inflammation: Evidence from in Vitro Study. *Animal Cells and Systems* **2018**, *22* (1), 7–14. <https://doi.org/10.1080/19768354.2017.1405072>.
- (36) Guan, S.; Jia, B.; Chao, K.; Zhu, X.; Tang, J.; Li, M.; Wu, L.; Xing, L.; Liu, K.; Zhang, L.; Wang, X.; Gao, X.; Huang, M. UPLC–QTOF-MS-Based Plasma Lipidomic Profiling Reveals Biomarkers for Inflammatory Bowel Disease Diagnosis. *J. Proteome Res.* **2020**, *19* (2), 600–609. <https://doi.org/10.1021/acs.jproteome.9b00440>.
- (37) Calzada, E.; Onguka, O.; Claypool, S. M. Phosphatidylethanolamine Metabolism in Health and Disease. *Int Rev Cell Mol Biol* **2016**, *321*, 29–88. <https://doi.org/10.1016/bs.ircmb.2015.10.001>.
- (38) Hamoud, A.-R.; Weaver, L.; Stec, D. E.; Hinds, T. D. Bilirubin in the Liver–Gut Signaling Axis. *Trends in Endocrinology & Metabolism* **2018**, *29* (3), 140–150. <https://doi.org/10.1016/j.tem.2018.01.002>.
- (39) Guan, Z.; Tian, B.; Perfumo, A.; Goldfine, H. The Polar Lipids of *Clostridium Psychrophilum*, an Anaerobic Psychrophile. *Biochim Biophys Acta* **2013**, *1831* (6), 1108–1112. <https://doi.org/10.1016/j.bbalip.2013.02.004>.
- (40) Tian, B.; Guan, Z.; Goldfine, H. Ethanolamine-Phosphate Modified Glycolipids in *Clostridium Acetobutylicum* That Respond to Membrane Stress. *Biochim Biophys Acta* **2013**, *1831* (6), 1185–1190. <https://doi.org/10.1016/j.bbalip.2013.03.005>.
- (41) Winston, J. A.; Theriot, C. M. Diversification of Host Bile Acids by Members of the Gut Microbiota. *Gut Microbes* **2019**, *11* (2), 158–171. <https://doi.org/10.1080/19490976.2019.1674124>.
- (42) Winter, S. E.; Thiennimitr, P.; Winter, M. G.; Butler, B. P.; Huseby, D. L.; Crawford, R. W.; Russell, J. M.; Bevins, C. L.; Adams, L. G.; Tsolis, R. M.; Roth, J. R.; Bäumler, A. J. Gut Inflammation Provides a Respiratory Electron Acceptor for *Salmonella*. *Nature* **2010**, *467* (7314), 426–429. <https://doi.org/10.1038/nature09415>.
- (43) Thiennimitr, P.; Winter, S. E.; Winter, M. G.; Xavier, M. N.; Tolstikov, V.; Huseby, D. L.; Sterzenbach, T.; Tsolis, R. M.; Roth, J. R.; Bäumler, A. J. Intestinal Inflammation Allows *Salmonella* to Use Ethanolamine to Compete with the Microbiota. *Proceedings of the National Academy of Sciences* **2011**, *108* (42), 17480–17485. <https://doi.org/10.1073/pnas.1107857108>.

- (44) Khan, C. M. A. The Dynamic Interactions between Salmonella and the Microbiota, within the Challenging Niche of the Gastrointestinal Tract. *Int Sch Res Notices* **2014**, *2014*, 846049. <https://doi.org/10.1155/2014/846049>.
- (45) Antunes, L. Caetano. M.; Andersen, S. K.; Menendez, A.; Arena, E. T.; Han, J.; Ferreira, R. B. R.; Borchers, C. H.; Finlay, B. B. Metabolomics Reveals Phospholipids as Important Nutrient Sources during Salmonella Growth in Bile In Vitro and In Vivo <sup>▽</sup>. *J Bacteriol* **2011**, *193* (18), 4719–4725. <https://doi.org/10.1128/JB.05132-11>.
- (46) Hendriks, T.; Schnabl, B. Indoles: Metabolites Produced by Intestinal Bacteria Capable of Controlling Liver Disease Manifestation. *Journal of Internal Medicine* **2019**, *286* (1), 32–40. <https://doi.org/10.1111/joim.12892>.
- (47) Shen, J.; Yang, L.; You, K.; Chen, T.; Su, Z.; Cui, Z.; Wang, M.; Zhang, W.; Liu, B.; Zhou, K.; Lu, H. Indole-3-Acetic Acid Alters Intestinal Microbiota and Alleviates Ankylosing Spondylitis in Mice. *Frontiers in Immunology* **2022**, *13*.
- (48) Liu, L.; Yang, M.; Dong, W.; Liu, T.; Song, X.; Gu, Y.; Wang, S.; Liu, Y.; Abla, Z.; Qiao, X.; Liu, W.; Jiang, K.; Wang, B.; Zhang, J.; Cao, H. Gut Dysbiosis and Abnormal Bile Acid Metabolism in Colitis-Associated Cancer. *Gastroenterol Res Pract* **2021**, *2021*, 6645970. <https://doi.org/10.1155/2021/6645970>.
- (49) Choi, S.-C.; Brown, J.; Gong, M.; Ge, Y.; Zadeh, M.; Li, W.; Croker, B. P.; Michailidis, G.; Garrett, T. J.; Mohamadzadeh, M.; Morel, L. Gut Microbiota Dysbiosis and Altered Tryptophan Catabolism Contribute to Autoimmunity in Lupus-Susceptible Mice. *Sci Transl Med* **2020**, *12* (551), eaax2220. <https://doi.org/10.1126/scitranslmed.aax2220>.
- (50) Zhang, Y.; Li, M.; Pu, Z.; Chi, X.; Yang, J. Multi-Omics Data Reveals the Disturbance of Glycerophospholipid Metabolism and Linoleic Acid Metabolism Caused by Disordered Gut Microbiota in PM2.5 Gastrointestinal Exposed Rats. *Ecotoxicology and Environmental Safety* **2023**, *262*, 115182. <https://doi.org/10.1016/j.ecoenv.2023.115182>.